Macro-Ripple Phase Formation in Bilayers Composed of Galactosylceramide and Phosphatidylcholine

Rhoderick E. Brown, Wayne H. Anderson, and Vitthal S. Kulkarni
The Hormel Institute, University of Minnesota, Austin, Minnesota 55912-3698 USA

ABSTRACT As determined by freeze fracture electron microscopy, increasing levels of bovine brain galactosylceramide (GalCer) altered the surface structure of 1-palmitoyl-2-oleoyl-phosphatidylcholine (POPC) bilayers by inducing a striking "macro-ripple" phase in the larger, multilamellar lipid vesicles at GalCer mole fractions between 0.4 and 0.8. The term "macro-ripple" phase was used to distinguish it from the $P_{\beta'}$ ripple phase observed in saturated, symmetric-chain length phosphatidylcholines. Whereas the $P_{\beta'}$ ripple phase displays two types of corrugations, one with a wavelength of 12–15 nm and the other with a wavelength of 25–35 nm, the macro-ripple phase occurring in GalCer/POPC dispersions was of one type with a wavelength of 100–110 nm. Also, in contrast to the extended linear arrays of adjacent ripples observed in the $P_{\beta'}$ ripple phase, the macro-ripple phase of GalCer/POPC dispersions was interrupted frequently by packing defects resulting from double dislocations and various disclinations and, thus, appeared to be continuously twisting and turning. Control experiments verified that the macro-ripple phase was not an artifact of incomplete lipid mixing or demixing during preparation. Three different methods of lipid mixing were compared: a spray method of rapid solvent evaporation, a sublimation method of solvent removal, and solvent removal using a rotary evaporation apparatus. Control experiments also revealed that the macro-ripple phase was observed regardless of whether lipid specimens were prepared by either ultra-rapid or manual plunge freezing methods as well as either in the presence or absence of the cryo-protectant glycerol. The macro-ripple phase was always observed in mixtures that were fully annealed by incubation above the main thermal transition of both POPC and bovine brain GalCer before rapid freezing. If the GalCer mixed with POPC contained only nonhydroxy acyl chains or only 2-hydroxy acyl chains, then the occurrence of macro-ripple phase decreased dramatically.

INTRODUCTION

Recent developments using lipid self-assemblies as templates to produce rugged, stable nano- and microstructures by metallization techniques have stimulated interest in lipid morphology (Schnur, 1993). As a result, much attention has been focused on the hollow bilayer tubules formed by diacetylenic phospholipids and on the cochleate bilayer cylinders formed by certain monoglycosylated sphingolipids. To gain insight into the hydration parameters affecting glycolipid microstructural morphology, the morphology of pure bovine brain galactosylceramide (GalCer) and its subfractions containing either 2-hydroxylated (HFA-GalCer) or nonhydroxylated acyl chains (NFA-GalCer) (see Fig. 1) has been investigated in aqueous and different nonaqueous solvents (Archibald and Yager, 1992; Schoen et al., 1993). Aside from their potential applications within the molecular engineering field, monoglycosylated sphingolipids like GalCer are of biomedical importance because of the essential structural roles they play in specialized biological membranes like myelin, brush border membranes of kidney and intestinal epithelial cells, and granular epidermis. These membranes possess unique functional properties due, in large part, to the structural stability provided by the presence of simple glycosphingolipids like GalCer. Proper membrane function requires that these glycosphingolipids not only be present, but that their relative content be optimized. In fact, myelin function is impaired if GalCer content is too low, as is the case in Pelizaeius-Merzbacher's disease (Witter et al., 1980) or if GalCer content grossly exceeds optimum levels, as is the case in globoid cell leukodystrophy (e.g., Suzuki and Suzuki, 1989). Optimal GalCer content in myelin is also thought to be a key factor in the unusually low proton permeability of myelin lipid bilayers (Diaz and Monreal, 1994). The molecular basis for these essential structural roles is poorly understood. Other recently discovered functional roles for GalCer have important implications in virology. This sphingolipid can serve as a cell surface receptor for the gp120 glycoprotein of type 1 HIV in $CD4^-$ cells (Harouse et al., 1991; Bhat et al., 1991). Also, GalCer and other sphingolipids recently have been shown to be essential components in target membranes for the low pH-induced fusion activity of Semliki Forest virus to occur (Nieva et al., 1994). These findings have sparked new interest in understanding the parameters governing GalCer's accessibility at the membrane surface.

Received for publication 18 July 1994 and in final form 5 January 1995.

Address reprint requests to Dr. Rhoderick E. Brown, The Hormel Institute, University of Minnesota, 801 16th Avenue NE, Austin, MN 55912. Tel.: 507-433-8804; Fax: 507-437-9606; E-mail: reb@maroon.tc.umn.edu.

Portions of this investigation were presented at the Fogarty International Center's Conference on *Domain Organization in Biological Membranes* held at NIH, Bethesda, MD on March 2–4, 1994.

Abbreviations used: GalCer, galactosylceramide; POPC, 1-palmitoyl-2-oleoyl-*sn*-glycero-3-phosphocholine; DPPC, dipalmitoyl-*sn*-glycero-3-phosphocholine; DMPC, dimyristoyl-*sn*-glycero-3-phosphocholine; SOPC, 1-stearoyl-2-oleoyl-*sn*-glycero-3-phosphocholine; EM, electron microscopy; GalSpd, deacylated GalCer with naturally occurring sphingoid bases, usually sphingosine (≈90%) and dihydrosphingosine (≈10%)

0006-3495/95/04/1396/10 $2.00

A number of investigators have noted that GalCer has rather unusual physical properties compared with glycerol-based phospholipids (for reviews, see Maggio, 1994; Curatolo, 1987; Thompson and Tillack, 1985). These unusual properties have been attributed, at least in part, to GalCer's ability to form intermolecular hydrogen bonds (e.g., Bunow and Levin (1980) and Pink et al. (1988)). Although the basic structural motif of GalCer is that of a lamellar bilayer assembly (e.g., Pascher and Sundell, 1977; Ruocco et al., 1981; Reed and Shipley, 1987; Pascher et al., 1992), this monoglycosylated sphingolipid has the capacity to form extraordinarily stable lamellar crystalline phases near physiological temperature (Bunow, 1979; Curatolo, 1982; Curatolo and Jungalwala, 1985; Lee et al., 1986). Other metastable, gel-like phases also have been reported in bovine brain GalCer, providing the possibility for the coexistence of multiple lateral domains enriched in various GalCer species (Jackson et al., 1988). Interestingly, manipulations of GalCer's acyl chain length (e.g., palmitate (16:0), stearate (18:0), or lignocerate (24:0)) produce little change in the high enthalpy, lamellar crystal-to-liquid crystal phase transition temperature that occurs near 80°C (Ruocco et al., 1983; Curatolo and Jungalwala, 1985; Reed and Shipley, 1987, 1989). The presence of 2-hydroxy acyl chains in naturally occurring GalCer (40–50 mole%) is thought to prevent formation of the lamellar crystal phase at physiologic temperatures by interfering with the dehydration event necessary to achieve it (Curatolo, 1987). Not surprisingly, the mixing behavior of phosphatidylcholines with naturally occurring GalCer or with its NFA- and HFA-subfractions is complex as revealed by Raman spectroscopic (Bunow and Levin, 1980), by calorimetric (Ruocco et al., 1983; Curatolo, 1986; Bunow and Levin, 1988; Johnston and Chapman, 1988; Gardam and Silvius, 1989), by fluorescence (Rintoul and Welti, 1989), by monolayer (Ali et al., 1991), and by NMR techniques (Neuringer et al., 1979; Morrow et al., 1992; Lu et al., 1993). What is not clear is whether the complexity of the mixing is reflected in the surface morphology of GalCer/phosphatidylcholine bilayers.

Here we show by freeze fracture electron microscopy that increasing GalCer content induces dramatic changes in the surface structure of PC bilayers, including formation of a composition-dependent macro-ripple phase. The physical characteristics of this macro-ripple phase are compared with those of the ripple structure that occurs in the $P_{\beta'}$ phase of saturated-chain phosphatidylcholines. Furthermore, we show that the macro-ripple phase formation depends on GalCer, with both 2-hydroxy and nonhydroxy acyl chains being present in the POPC mixtures.

MATERIALS AND METHODS

1-palmitoyl-2-oleoyl phosphatidylcholine (POPC) and bovine brain GalCer containing both nonhydroxy (≈60%) and 2-hydroxy (≈40%) fatty acyl chains were obtained from Avanti Polar Lipids (Alabaster, AL). GalCer containing either 99% nonhydroxy fatty acyl chains (NFA) or 99% 2-hydroxy acyl chains (HFA) was purchased from Sigma Chemical Co. (St. Louis, MO). The fatty acyl composition of all three GalCer fractions has been reported previously (Johnson and Brown, 1992). GalCer possesses an abundance of lignoceroyl (24:0), nervonoyl (24:$1^{\Delta 15(cis)}$), 2-hydroxy lignoceroyl (2-OH 24:0), 2-hydroxy behenoyl (2-OH 22:0), and 2-hydroxy nervonoyl (2-OH 24:$1^{\Delta 15(cis)}$) acyl residues coupled via an amide linkage to an

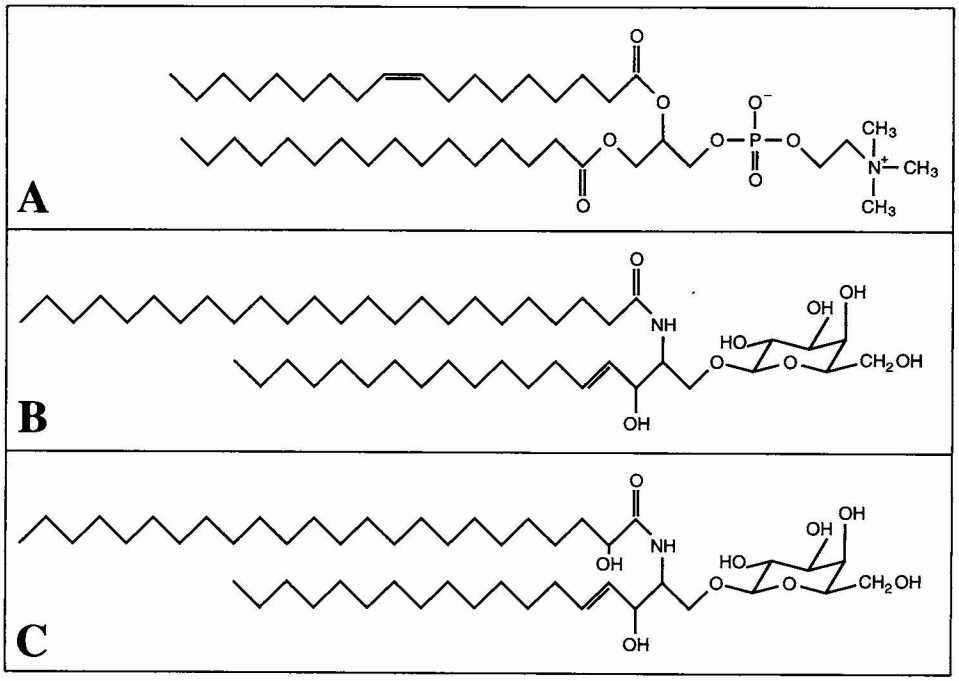

FIGURE 1 Structural configuration of phosphatidylcholine and galactosylceramide. (*A*) 1-palmitoyl-2-oleoyl phosphatidylcholine (POPC). (*B*) GalCer containing a lignoceroyl (C 24:0) acyl chain representing a commonly occurring NFA-GalCer found in bovine brain. (*C*) GalCer containing a cerebronoyl (2-OH 24:0) acyl chain representing a commonly occurring HFA-GalCer found in bovine brain.

18-carbon sphingoid base (Fig. 1). Lipid purity was over 99% as determined by thin layer chromatography using $CHCl_3/CH_3OH/-H_2O$ (50:21:3) followed by charring with chromic-sulfuric acid spray or by fluorescence illumination after spraying with primulin. No breakdown of either POPC or GalCer was detectable after hydration and dispersion by the procedures described below.

Preparation of lipid dispersions

Lipid mixtures were prepared by three different methods. In the first method, GalCer and POPC were co-dissolved in $CHCl_3/CH_3OH$ and the solvent was removed by rotary evaporation. Remaining traces of solvent were evaporated by subjecting samples to reduced pressure (using a vacuum pump) for 2 h. Because demixing of different lipids can occur if solvent evaporation is slow (e.g., Thompson et al., 1985), we also made use of two other methods designed to prevent artifactual demixing of lipids. In one, a spray method was used that provides near instantaneous removal of the majority of solvent (see Thompson et al., 1985). In our case, we used an Iwata airbrush (model HP-SB; Medea Trading Co., Portland, OR) with nitrogen as the propellant to produce an aerosol of the lipid/solvent mix. The aerosol was sprayed onto a clean glass plate that was then subjected to reduced pressure (using a vacuum pump) for 2 h. Alternatively, lipid mixing was ensured using a variation of the sublimation method developed by Lin and Huang (1988). Briefly, the lipids were mixed from their stock solutions of $CHCl_3/CH_3OH$, and the solvent was removed under a stream of nitrogen. The lipid film was redissolved by vortexing in 0.2 ml of 2-methyl-2- propanol and warmed with tap water (~50°C) to achieve a clear solution. Then the sample was frozen rapidly by submerging in isopropanol cooled by dry ice. Lyophilization of the solid 2-methyl-2-propanol resulted in a dry lipid mix.

In all cases, samples were hydrated with buffer comprised of 10 mM HEPES (pH 7.2) containing 150 mM NaCl, 1.0 mM Na_2EDTA, and 0.02% NaN_3. Immediately after adding buffer, samples were heated to 90°C and were vortexed vigorously for 1 min. Three more cycles of heating and vortexing followed, and then samples were heated for an additional 5 min. The heating step was performed to assure mixing above the phase transition temperature of both lipids. Then samples were allowed to sit overnight at room temperature before EM analysis.

Freeze-fracture electron microscopy

Small aliquots of lipid dispersions were placed on gold alloy specimen holders at room temperature and then frozen by plunging into either liquid Freon 22 or liquid propane cooled by liquid nitrogen. In later studies, samples were frozen using the Controlled Environment Vitrification System (CEVS), in which samples were maintained under a humidified atmosphere to minimize the possibility of evaporative artifacts and then plunged into liquid propane to achieve ultra-rapid freezing (Bellare et al., 1988). In this case, a copper sandwich sample holder was used. Replicas were produced as described previously (Brown and Hyland, 1992) by fracturing specimens at −110°C in a Balzers BAF300 freeze-fracture apparatus equipped with a electron guns for Pt/C shadowcasting (45° angle) and for depositing carbon support films. Replicas were floated onto distilled water, retrieved on untreated 200-mesh copper grids, and cleaned with $CHCl_3/CH_3OH$ (2:1) to remove residual lipid before being examined in a JEOL 100-S transmission electron microscope.

RESULTS

Early morphological studies clearly demonstrated the similarity between the abnormal cellular inclusions characteristic of globoid cell leukodystrophy and negatively stained brain GalCer (Yunis and Lee, 1970). Subsequent studies of GalCer/dipalmitoyl phosphatidylcholine (DPPC) aqueous dispersions at a few mixing ratios indicated that elevation of GalCer levels does alter the average morphological size of PC liposomes (Curatolo and Neuringer, 1986; Maggio et al., 1988). These negative-stain EM studies provided no indication as to whether GalCer affects the surface structure of PC lipid dispersions.

To determine the effect of increasing GalCer content on the surface structure of POPC, we investigated using the freeze fracture electron microscopic technique (Figs. 2 and 3). Freeze-fracture EM is well suited for visualizing the surface features in lipid dispersions (for review, see Sternberg, 1992). In the absence of GalCer, the POPC liposomes displayed relatively smooth surfaces, which are typical of the liquid crystalline state (Fig. 2 *A*). However, at GalCer mole fractions of 0.1 and 0.2, the surface structure of larger liposomes showed irregularities consisting of shallow depressions and connected "blister-like" protrusions (Fig. 2 *B*). At GalCer mole fractions of 0.3 and 0.4, the surface structures of the large liposomes began to show occasional regions with tubular undulations (Fig. 2 *C*). At GalCer mole fractions above 0.4 but below 0.8, the occasional and random undulations transformed into a striking and symmetric ripple phase (Figs. 2 *D* and 3 *A–C*). Edge fractures revealed that the ripples in adjacent lamellae appeared to be in register and persisted through many concentric, bilayer stacks (Fig. 6 *A*). Careful examination of many micrographs revealed that the macro-ripple phase was confined to the larger, multilamellar vesicles of the hydrated dispersions and generally was not seen when the vesicle diameter diminished to less than 1000 nm. Although the number of smaller vesicles far exceeded the larger rippled vesicles, the total lipid mass committed to macro-rippling appeared to exceed that in the smaller non-rippled vesicles because of the large size and high lamellarity in the macro-rippled vesicles. Because GalCer mole fractions exceeding 0.3 promoted aggregation of the lipid dispersions, we were unable to assess accurately the exact percentage of lipid involved in macro-rippling. Figs. 2 *D* and 3 *A–C* do provide some indication of the variation in surface morphology observed in different size vesicles. Note that differences in the surface texture among large and small vesicles also has been reported for bovine brain sphingomyelin dispersions incubated at temperatures where both liquid crystalline and gel phase coexist (Döbereiner et al., 1993). Interestingly, all traces of the ripple phase vanished when POPC was absent, and only GalCer was present regardless of vesicle size (Fig. 3 *D*). Pure GalCer surfaces appeared smooth, often exhibiting tightly packed, concentric bilayer stacks in cross section (Fig. 3 *D*, *lower left*).

Several control experiments were performed to verify the results shown in the electron micrographs. To determine whether the observed ripple phase was the result of incomplete mixing before hydration of the lipid dispersions, we compared the spray method of solvent evaporation (Thompson et al., 1985), the sublimation method of solvent removal (Lin and Huang, 1988), and conventional solvent removal by rotary evaporation (see Materials and Methods for details). The importance of sample preparation on the observed mixing behavior was clearly pointed out in freeze fracture studies involving ganglioside mixing with POPC

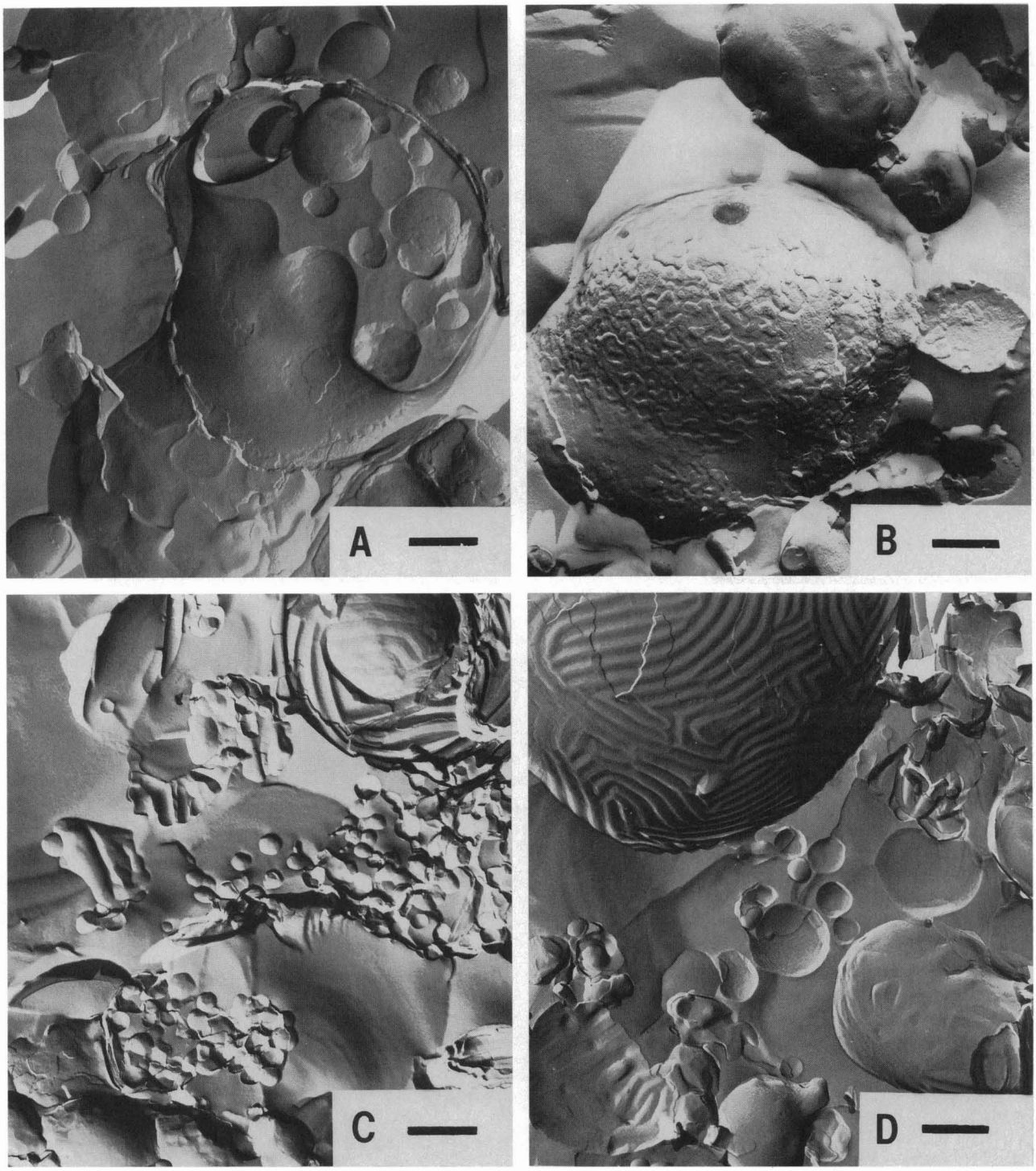

FIGURE 2 Effect of increasing GalCer content on the surface morphology of aqueous GalCer/POPC dispersions. The bar in the lower right corner of each panel represents 400 nm. The GalCer mole fractions in the GalCer/POPC dispersions are zero in *A*, 0.2 in *B*, 0.4 in *C*, and 0.5 in *D*. Samples were quick-frozen from room temperature (~22°C) by plunging into liquid propane after preparing as described in Materials and Methods.

(Thompson et al., 1985) and in differential scanning calorimetric studies of binary mixtures of PC molecular species (Lin and Huang, 1988). Our results showed that both the spray method and the sublimation method of solvent removal produced dispersions with fairly uniform surface characteristics, including the striking ripple phase within the appropriate GalCer/POPC mole fractional range. In contrast, samples prepared by conventional rotary evaporation showed more variation in their surface characteristics (data not shown). The chief advantage of the sublimation method over the spray method of solvent removal was in sample recovery. We found that with the spray method sample

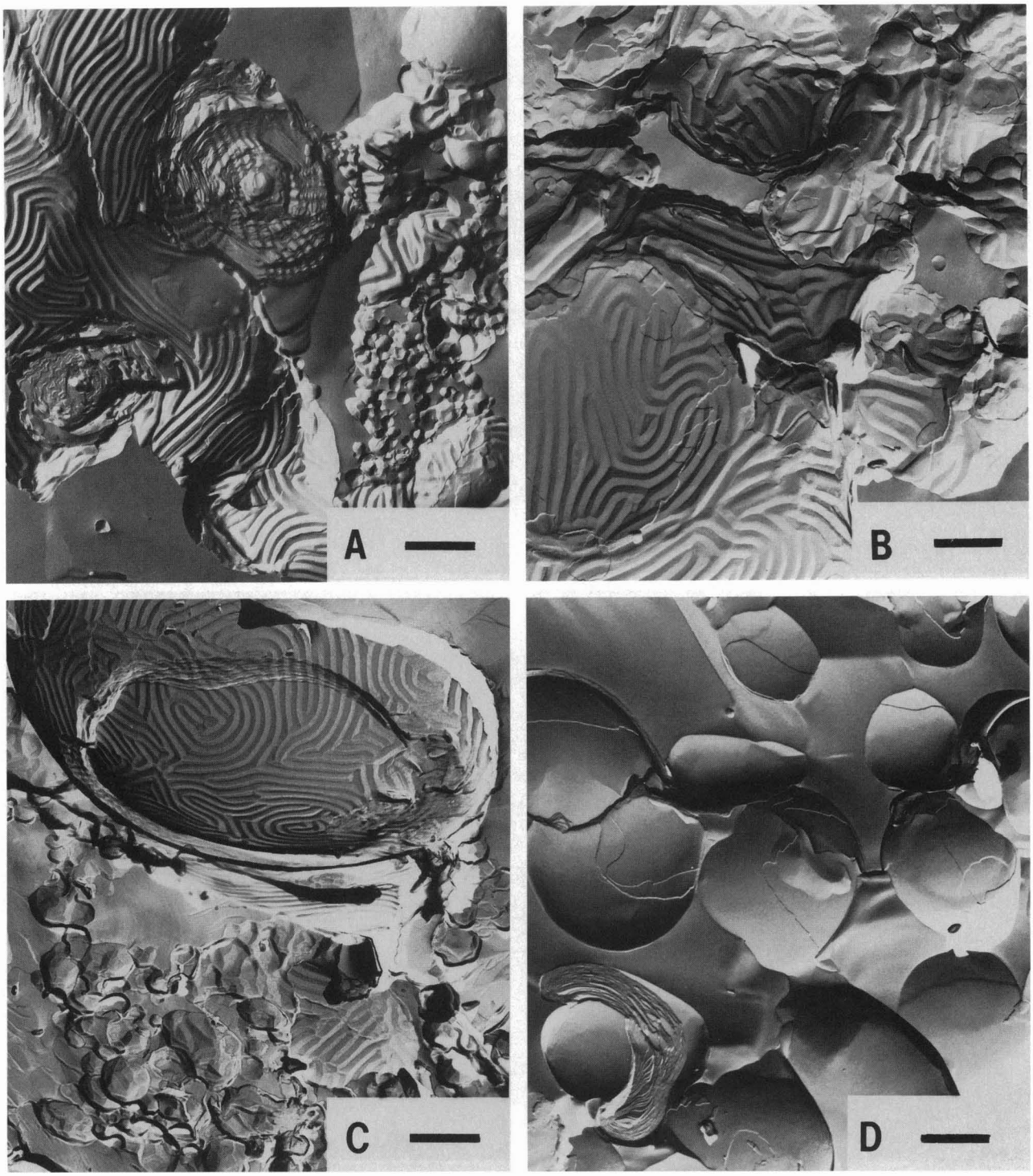

FIGURE 3 Effect of increasing GalCer content on the surface morphology of aqueous GalCer/POPC dispersions. The bar in the lower right corner represents 700 nm in *A* and *C* and represents 400 nm in *B* and *D*. The GalCer mole fractions in the GalCer/POPC dispersions are 0.6 in *A*, 0.7 in *B*, 0.8 in *C*, and 1.0 in *D*. Samples were quick-frozen from room temperature (~22°C) by plunging into liquid propane after preparing as described in Materials and Methods.

recovery varied according to a number of factors, including propellant pressure, distance of sprayer from the glass plate, and lipid composition. These factors combined to make recovery of samples quite variable. In contrast, the sublimation method of solvent removal permitted recovery of virtually all of the sample with less manual manipulation.

To determine whether freezing rate affected macro-ripple phase formation, we compared samples prepared by manual plunge freezing into either liquid Freon or liquid propane and ultra-rapid plunge freezing into liquid propane using the CEVS (see Materials and Methods for details). In every instance, macro-ripple phase was observed in the large vesicles

when GalCer mole fractions were between 0.4 and 0.8. Thus, it was clear that the ripple phase in bovine brain GalCer/POPC mixtures was not an artifact due to sample unmixing caused by "slow" freezing. Ripple-phase formation also occurred regardless of whether the cryo-protectant glycerol was present during sample freezing. We found this result to be interesting because of glycerol's known ability to promote transbilayer interdigitation in lamellar assemblies of certain phospholipids (e.g., McDaniel et al., (1983)). Although glycerol had no apparent effect on whether macro-ripple phase formed, the presence of this cryo-protectant did result in pure GalCer having a faceted, plate-like appearance rather than the smooth surfaces that occurred in glycerol's absence (Fig. 3 *D* vs. 4 *A*). The only experimental condition that resulted in no ripple-phase formation at X_{GalCer} between 0.4 and 0.8 was hydrating and vortexing the dispersions at room temperature and omitting the warming step. In this instance, multilamellar aggregates formed that resembled clusters of partially fused liposomes with diameters between 120 and 150 nm (Fig. 4 *B*).

Effect of GalCer acyl structure on the macro-ripple phase

To determine the role that GalCer's 2-hydroxy acyl chains play in determining surface structure, we studied POPC mixtures containing various amounts of two different GalCer subfractions, one containing only 2-hydroxy acyl chains and the other containing only nonhydroxy acyl chains. Despite investigating a broad range of NFA-GalCer/POPC and HFA-GalCer/-POPC, very little macro-ripple phase was seen. Fig. 5, *A* and *B* show replicas of POPC dispersions containing either 70 mol% NFA-GalCer or 60 mol% HFA-GalCer, respectively. Instead of extended surface areas showing macro-ripple phase, dispersions containing high levels of NFA-GalCer (Fig. 5 *A*) showed occasional tubule-like structures among larger plate-like assemblies. The tubular structures had a diameter of about 30 nm. Curiously, samples containing large amounts of NFA-GalCer proved difficult to fracture effectively. Repeated attempts revealed that specimen fracturing was restricted largely to cruxic boundaries between large ice crystals. Whether this behavior is a consequence of transbilayer interdigitation of acyl chains and the extremely tight lateral packing of NFA-GalCer will require further study. Although deep etching may provide a way to reveal more sample surface, the image shown in Fig. 5 *A* was representative of what we observed under the fracturing conditions to which all samples were subjected. In contrast, POPC mixtures containing HFA-GalCer resembled partially fused or aggregated liposomes with diameters varying from 300 to 600 nm and distributed in random clusters throughout the ice with little evidence of macro-ripple phase (Fig. 5 *B*).

Characterization of the macro-ripple phase

The macro-ripple phase associated with bovine brain GalCer/POPC mixtures differed in many ways from the well studied ripple phase associated with the $P_{\beta'}$ phase of saturated-chain

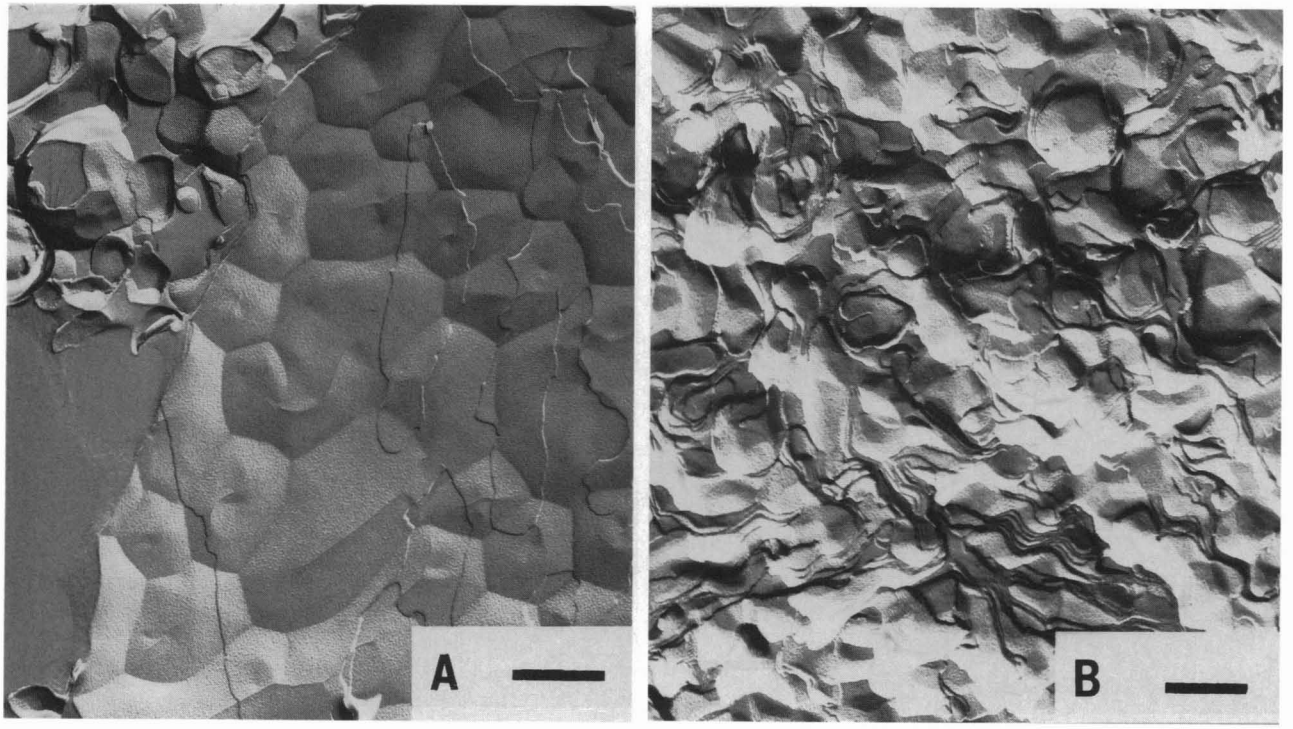

FIGURE 4 Effect of glycerol and incubation temperature on surface morphology. The bar in the lower right corner of *A* represents 300 nm and in *B*, 200 nm. (*A*) Pure GalCer dispersions that have been quick-frozen in the presence of glycerol (compare with Fig. 3 *D* in which no glycerol is present). (*B*) Mixtures containing 0.5 mole fraction of GalCer. The incubation step at 90°C was omitted before quick-freezing from room temperature, and no macro-ripple phase was observed.

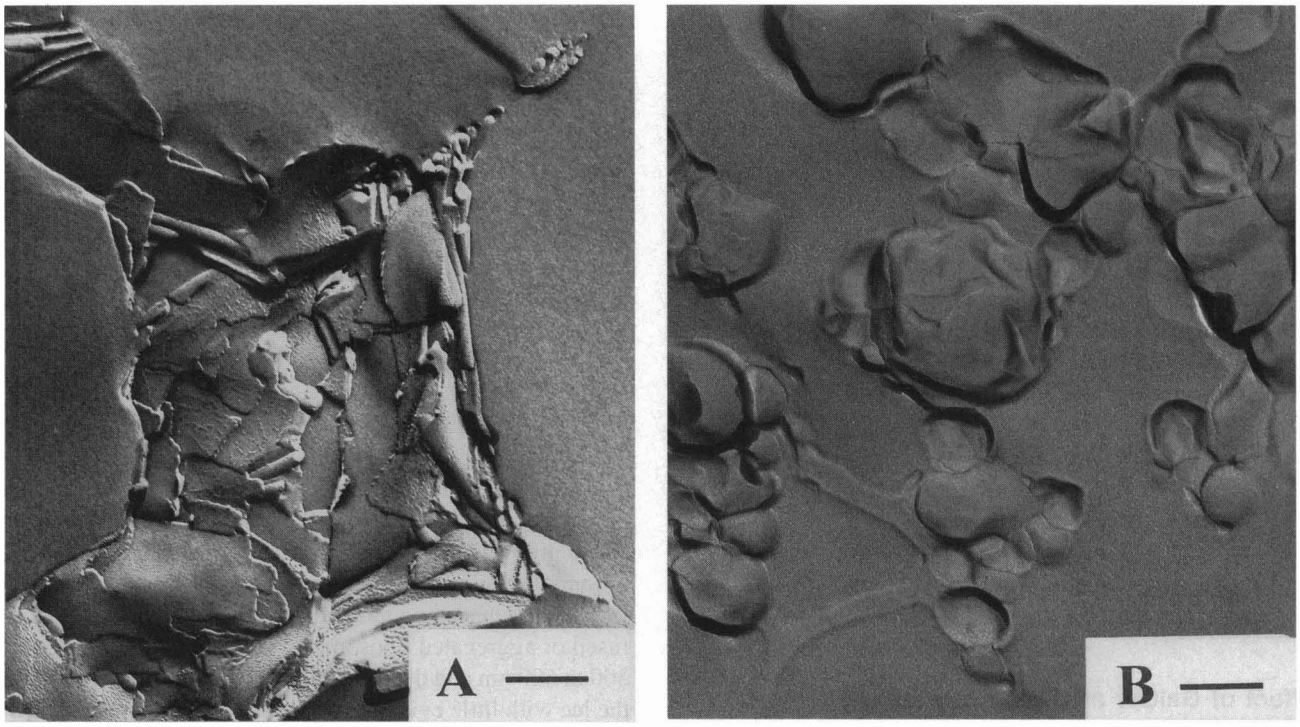

FIGURE 5 Effect of NFA-GalCer and HFA-GalCer on surface morphology. The bar in the lower right corner of *A* represents 200 nm and in *B*, 200 nm. (*A*) Aqueous mixtures containing 0.7 mole fraction of NFA-GalCer in POPC. Note the occasional tubule-like structures. (*B*) Aqueous mixtures containing 0.6 mole fraction of HFA-GalCer in POPC.

phosphatidylcholines, which is shown in Fig. 6 *B* (e.g., Janiak et al., 1976; Tillack et al., 1982; Hicks et al., 1987). GalCer/POPC dispersions displayed only one type of corrugation or ripple, a symmetric macro-ripple with a wave-

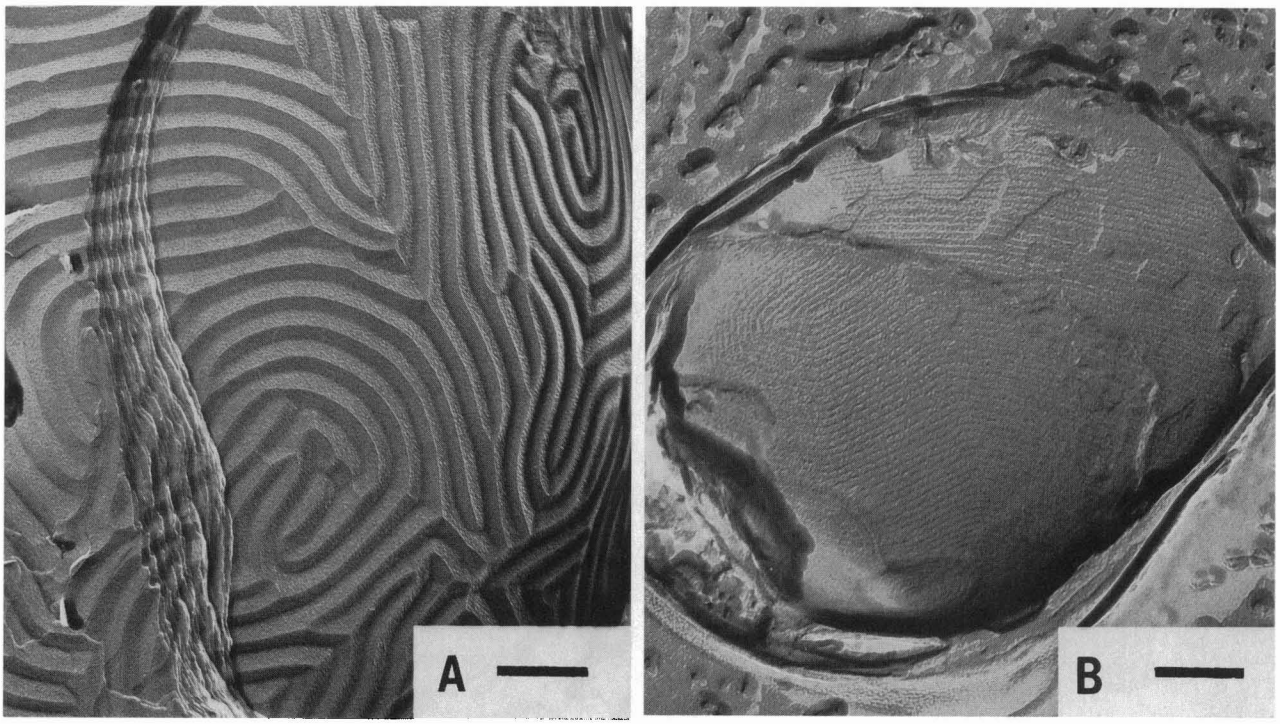

FIGURE 6 Comparison of macro-ripple in GalCer/POPC dispersions and the $P_{\beta'}$ ripple phase of DMPC. The bar in the lower right corner of *A* represents 300 nm and in *B*, 150 nm. (*A*) High magnification view of the macro-ripple phase in GalCer/POPC dispersions containing 0.8 mole fraction GalCer. (*B*) $P_{\beta'}$ ripple phase that occurs in DMPC dispersions quick-frozen from room temperature (~22°C).

length of 100–110 nm. The depth (amplitude) of the macro-ripple, as determined from occasional perpendicular cross sections, was ~30 (±5) nm. In contrast, the $P_{\beta'}$ phase is known to exhibit two different ripple structures, sometimes referred to as Λ corrugations and Λ/2 corrugations (Sackmann et al., 1980; Rüppel and Sackmann, 1983; Zasadzinski and Schneider, 1987; Hicks et al., 1987; Yao et al., 1991; Vinson et al., 1991). Λ/2 corrugations have an asymmetric modulation with a 12–15 nm wavelength, whereas, Λ corrugations possess a symmetric modulation with spacing periodicities of 22–26 nm. The amplitudes of the Λ and Λ/2 ripples of PC are 9 and 4.5 nm, respectively (Zasadzinski and Schneider, 1987). Detailed examination of Λ corrugations has led to various structural models including the "W" model (Sackmann et al., 1980; Zasadzinski and Schneider, 1987) in which a small peak is located in the center of a deep trough. In a recent variation of the "W" model, Vinson et al. (1991) suggested a more symmetric variation in which there is not only a small peak located in the center of a deep trough, but also a small trough located at the apex of each large peak. Hence, the physical dimensions of the macro-ripple phase in GalCer/POPC mixtures are significantly different from those associated with the $P_{\beta'}$ phase of saturated-chain PCs.

Fig. 6 *A* also illustrates the different types of defects that lead to changes in the surface profiles of GalCer/POPC mixtures. Extended linear arrays of adjacent ripples are rare and are often interrupted by various defects such as double dislocations, pairs of disclinations, and +1/2 disclinations (e.g., Sackmann et al., 1980). Also, grain boundaries are not observed. The net effect of these defects is to produce a nearly continually twisting and turning of the macro-ripple. This situation contrasts that of the $P_{\beta'}$ phase of saturated-chain phosphatidylcholines in which strikingly fewer defects interrupt the two ripple phases (Fig. 6 *B*). The $P_{\beta'}$ phase contains large regions characterized by long linear arrays of adjacent ripples aligned parallel to one another with only occasional +1/2 disclinations and 60° bends (Kleman, 1978; Rüppel and Sackmann, 1983; Zasadzinski and Schneider, 1987; Vinson et al., 1991). Long linear grain boundaries also are occasionally observed.

DISCUSSION

This study provides insight into the ultrastructural changes that increasing levels of GalCer impart to phosphatidylcholine model membranes. GalCer not only alters the size and shape of PC model membranes (Curatolo and Neuringer, 1986; Maggio et al., 1988) but also dramatically changes the surface structure of PC bilayers. Our freeze-fracture electron micrographs show that the most striking alteration in surface structure takes the form of a macro-ripple phase that forms in the large multilamellar vesicles of the dispersions. What is intriguing about the macro-ripple phase characterized in the present investigation is that it is a compositionally rather than thermally induced phase structure occurring in hydrated mixtures of a PC and GalCer possessing physiologically relevant hydrocarbon structures.

The molecular arrangement of lipids necessary for macro-ripple phase formation is not clear at the present time. The complexity of the mixtures in terms of acyl chain and headgroup heterogeneity makes molecular modeling unrealistic. Nevertheless, there are physical parameters characteristic of this mixed lipid system that probably contribute to macro-ripple phase formation. The mere presence of the macro-ripple phase does indicate nonideal mixing of the lipids and is consistent with immiscibility in the lipid mixture. This is not surprising given existing literature reports. Our interfacial studies of bovine brain GalCer and POPC mixed monolayers showed evidence of multiple transitions in force-area isotherms recorded at GalCer mole fractions between 0.4 and 0.8 (Ali et al., 1991). In the case of GalCer/POPC bilayer mixtures (Curatolo, 1986), differential scanning calorimetric studies provide evidence for the existence of substantial amounts of gel phase (highly enriched in GalCer) coexisiting with liquid-crystalline phase (relatively devoid of GalCer) under conditions where we observe the macro-ripple phase. Application of the lever rule to Curatolo's phase diagram at equimolar bovine brain GalCer and POPC and at room temperature (20°C) shows that the liquid-crystalline phase accounts for almost 40% of the total lipid but is comprised of about 95% POPC and only 5% GalCer. The gel phase accounts for 60% of the total lipid but contains about 15% POPC and 85% GalCer. Complex phase diagrams also have been reported for various GalCer subfractions and derivatives in mixtures with other PCs (e.g., Ruocco et al., 1983; Maggio et al., 1985; Johnston and Chapman, 1988; Rintoul and Welti, 1989; Gardam and Silvius, 1989), and it is clear that NFA-GalCer and HFA-GalCer do not mix in exactly the same way with egg PC (Bunow and Levin, 1988). In recent NMR studies, N-18:0 and N-24:0 GalCer derivatives displayed significant behavioral differences in SOPC bilayers (Morrow et al., 1992; Lu et al., 1993).

The lateral phase separation that occurs under the conditions where macro-ripple phase is observed is likely to be linked to GalCer's tendency to modulate curvature in PC bilayers. Indeed, the "intrinsic or spontaneous curvature" of different lipids has dramatic effects on shape changes that occur in mixed-composition membranes and is thought to be coupled to lipid phase separation (e.g., Sackmann, 1994; Siefert, 1993). Curvature-linked lipid phase separation is thought to affect both the lateral organization of lipids within a given bilayer leaflet as well as the transbilayer distributions of lipid mixtures. A consequence for GalCer/POPC mixtures could be the formation of a metastable structure with long-range order such as the macro-ripple phase, which reflects GalCer's tendency to form lipid tubules and cochleate myelinic cylinders. Indeed, structures of this nature have been reported when GalCer's environment is altered (Archibald and Yager, 1992; Schoen et al., 1993; Schnur, 1993) Recently, we have noted such morphology for certain NFA-GalCer molecular species in aqueous environments (our unpublished observations).

Although the complex mixing behavior that occurs in GalCer/POPC mixtures may be influenced by transbilayer acyl interdigitation of the sphingolipid (e.g., Melhourn et al., 1988), there is no compelling evidence at the present time to invoke transbilayer acyl chain interdigitation as being necessary for macro-ripple phase formation. Otherwise, extensive macro-ripple phase would also be expected in the HFA-GalCer/POPC and/or the NFA-GalCer/POPC mixtures. As noted above, the macro-ripple phase occurs extensively only when GalCer containing both 2-hydroxy and nonhydroxy acyl chains is present in the POPC. Typically, approximately equal amounts of NFA-GalCer and HFA-GalCer are present in bovine brain GalCer, and both the NFA-GalCer and HFA-GalCer are known to have mostly long acyl chains resulting in a large chain-length asymmetry (e.g., Johnson and Brown, 1992). Also, in agreement with our freeze-fracture micrographs of NFA-GalCer/POPC dispersions, Ruocco et al. (1983) reported no evidence of a ripple phase being present in hydrated dispersions of N-16:0 GalSpd/-DPPC mixtures, although a bilayer structural motif was maintained at all mixing ratios. Hence, other parameters must also play roles. One reasonable candidate appears to be the physico-chemical properties of the lipid polar region itself. In fact, many theories describing $P_{\beta'}$ ripple phase formation invoke not only the projected area mismatch of the hydrated polar headgroups and the hydrocarbon chains but also have suggested involvement of an order-disorder transition of lipid polar headgroups (Doniach, 1979; Pearce and Scott, 1982; Cevc, 1991). What is observed experimentally with saturated, chain-length symmetric PCs is that the molecules ripple in the $P_{\beta'}$ phase and tilt in the $L_{\beta'}$ phase.

With respect to GalCer, x-ray studies have revealed that *N*-24:0 GalSpd, N-18:0 GalSpd, and N-16:0 GalSpd are tilted about 21° from the bilayer normal position when in the extraordinarily stable liquid crystal bilayer phase (e.g., Reed and Shipley, 1987). However, the crystal phase of N-(2-OH)-18:0 GalSpd is tilted approximately 49° from the bilayer normal position (Pascher and Sundell, 1977). The added chain tilt most likely accommodates the expanded molecular area necessitated by the hydrogen-bonding network in which the HFA-GalCer headgroup and the 2-OH acyl group are involved (Bunow and Levin, 1980). This finding is consistent with the known influence that the lipid polar region's physicochemical properties has on the $P_{\beta'}$ ripple phase. For instance, demethylation of the PC headgroup eliminates the ripple phase. Mixtures of DMPC and DMPE bearing a monomethyl-substituted headgroup (DMPE-CH_3) show no evidence of a ripple phase when DMPE-CH_3 mole fraction exceeds 0.15 (Zasadzinski and Schneider, 1987).

In summary, it appears that complex interactions related to the structural parameters described above contribute to macro-ripple phase formation in bovine brain GalCer/POPC mixtures. More work with individual molecular species of GalCer that contain either nonhydroxy or 2-hydroxy acyl chains and with various PC molecular species is presently underway to define more clearly the essential structural elements controlling macro-ripple formation. Whether biological membrane preparations enriched in sphingolipids show evidence of rippling or other distinctive surface structural features is not resolved at present. Preliminary examination of sphingolipid-enriched membrane preparations from MDCK cells, i.e., caveolae (Sargiacomo et al., 1993), does show evidence of surface striations (our unpublished observations). However, more study will be needed to determine whether the sphingolipid or protein components are responsible for the surface striations.

We thank Sue Johnson for the expert technical assistance in preparing some of the lipid samples, Dr. Michael Lisanti for providing the caveolin-enriched membrane preparations, and Carmen Perleberg for spellchecking the manuscript.

This investigation, which received major support from U.S. Public Health Service grant GM45928 and the Hormel Foundation, benefited from a Small Instrumentation grant provided through the Division of Research Resources of National Institutes of Health for the CEVS ultra-rapid freezing device.

REFERENCES

Ali, S., H. L. Brockman, and R. E. Brown. 1991. Structural determinants of miscibility in surface films of galactosylceramide and phosphatidylcholine: effect of unsaturation in the galactosylceramide acyl chain. *Biochemistry.* 30:11198–11205.

Archibald, D. D., and P. Yager. 1992. Microstructural polymorphism in bovine brain galactocerebroside and its two major subfractions. *Biochemistry.* 31:9045–9055.

Bellare, J. R., H. T. Davis, L. E. Scriven, and Y. Talmon. 1988. Controlled environment vitrification system: an improved sample preparation technique. *J. Electron Microsc. Tech.* 10:87–111.

Bhat, S., S. L. Spitalnik, F. Gonzalez-Scarano, and D. H. Silberberg. 1991. Galactosyl ceramide or a derivative is an essential component of the neural receptor for human immunodeficiency virus type 1 envelope glycoprotein gp120. *Proc. Natl. Acad. Sci. USA.* 88:7131–7134.

Brown, R. E., and K. J. Hyland. 1992. Spontaneous transfer of ganglioside GM_1 from its micelles to lipid vesicles of differing size. *Biochemistry.* 31:10602–10609.

Bunow, M. R. 1979. Two gel states of cerebrosides: calorimetric and Raman spectroscopic evidence. *Biochim. Biophys. Acta.* 574:542–546.

Bunow, M. R., and I. W. Levin. 1980. Molecular conformations of cerebrosides in bilayers determined by Raman spectroscopy. *Biophys. J.* 32: 1007–1021.

Bunow, M. R., and I. W. Levin. 1988. Phase behavior of cerebroside and its fractions with phosphatidylcholines: calorimetric studies. *Biochim. Biophys. Acta.* 939:577–586.

Cevc, G. 1991. Polymorphism of bilayer membranes in the ordered phase and the molecular origin of lipid pretransition and rippled lamellae. *Biochim. Biophys. Acta.* 1062:59–69.

Curatolo, W. 1982. Thermal behavior of fractionated and unfractionated bovine brain cerebrosides. *Biochemistry.* 21:1761–1764.

Curatolo, W. 1986. The interactions of 1-palmitoyl-2-oleoyl phosphatidylcholine and bovine brain cerebroside. *Biochim. Biophys. Acta.* 861:373–376.

Curatolo, W. 1987. The physical properties of glycolipids. *Biochim. Biophys. Acta.* 906:111–136.

Curatolo, W., and F. B. Jungalwala. 1985. Phase behavior of galactocerebrosides from bovine brain. *Biochemistry.* 24:6608–6613.

Curatolo, W., and L. J. Neuringer. 1986. The effects of cerebrosides on model membrane shape. *J. Biol. Chem.* 261:17177–17182.

Diaz, R. S., and J. Monreal. 1994. Unusual low proton permeability of liposomes prepared from the endogenous myelin lipids. *J. Neurochem.* 62:2022–2029.

Döbereiner, H.-G., J. Käs, D. Noppl, I. Sprenger, and E. Sackmann. 1993. Budding and fission of vesicles. *Biophys. J.* 65:1396–1403.

Doniach, S. 1979. A thermodynamic model for the monoclinic (ripple) phase of hydrated lipid bilayers. *J. Chem. Phys.* 70:4587–4596.

Gardam, M., and J. R. Silvius. 1989. Intermixing of dipalmitoylphosphatidylcholine with phospho- and sphingolipids bearing highly asymmetric hydrocarbon chains. *Biochim. Biophys. Acta.* 980:319–325.

Harouse, J. M., S. Bhat, S. Spitalnik, S. L. Spitalnik, M. Laughlin, L. Stefano, and D. H. Silberberg. 1991. Inhibition of entry of HIV-1 in neural cell lines by antibodies against galactosyl ceramide. *Science.* 253:320–323.

Hicks, A., M. Dinda, and M. A. Singer. 1987. The ripple phase of phosphatidylcholines: effect of chain length and cholesterol. *Biochim. Biophys. Acta.* 903:177–185.

Jackson, M., D. S. Johnston, and D. Chapman. 1988. Differential scanning calorimetric and Fourier transform infrared spectroscopic investigations of cerebroside polymorphism. *Biochim. Biophys. Acta.* 944:497–506.

Janiak, M. J., D. M. Small, and G. G. Shipley. 1976. Nature of the thermal pretransition of synthetic phospholipids: dimyristoyl- and dipalmitoyllecithin. *Biochemistry.* 15:4575–4580.

Johnson, S. B., and R. E. Brown. 1992. Simplified derivatization for determining sphingolipid fatty acyl composition by gas chromatography-mass spectrometry. *J. Chromatogr.* 605:281–286.

Johnston, D. S., and D. Chapman. 1988. A calorimetric study of the thermodynamic behaviour of mixtures of brain cerebrosides with other brain lipids. *Biochim. Biophys. Acta.* 939:603–614.

Kleman, M. 1978. Defects in mesomorphic phases: theoretical aspects. *J. Microsc. Spectr. Electron.* 3:357–371.

Lee, D. C., I. R. Miller, and D. Chapman. 1986. An infrared spectroscopic study of metastable and stable forms of hydrated cerebroside bilayers. *Biochim. Biophys. Acta.* 859:266–270.

Lin, H., and C. Huang. 1988. Eutectic phase behavior of 1-stearoyl-2-capryl phosphatidylcholine and dimyristoylphosphatidylcholine mixtures. *Biochim. Biophys. Acta.* 946:178–184.

Lu, D., D. Singh, M. R. Morrow, and C. W. M. Grant. 1993. Effect of glycosphingolipid fatty acid chain length on behavior in unsaturated phosphatidylcholine bilayers: a ^{2}H NMR study. *Biochemistry.* 32:290–297.

Maggio, B. 1994. The surface behavior of glycosphingolipids in biomembranes: a new frontier of molecular ecology. *Prog. Biophys. Mol. Biol.* 62:55–117.

Maggio, B., J. Albert, and R. K. Yu. 1988. Thermodynamic-geometric correlations for the morphology of self-assembled structures of glycosphingolipids and their mixtures with dipalmitoylphosphatidylcholine. *Biochim. Biophys. Acta.* 945:145–160.

Maggio, B., T. Ariga, J. M. Sturtevant, and R. K. Yu. 1985. Thermotropic behavior of binary mixtures of dipalmitoylphosphatidylcholine and glycosphingolipids in aqueous dispersions. *Biochim. Biophys. Acta.* 818:1–12.

McDaniel, R. V., T. J. McIntosh, and S. A. Simon. 1983. Nonelectrolyte substitution for water in phosphatidylcholine bilayers. *Biochim. Biophys. Acta.* 731:97–108.

Melhorn, I. E., E. Florio, K. R. Barber, C. Lordo, and C. W. M. Grant. 1988. Evidence that transbilayer interdigitation of glycosphingolipid long chain fatty acids may be a general phenomenon. *Biochim. Biophys. Acta.* 939:151–159.

Morrow, M. R., D. Singh, D. Lu, and C. W. M. Grant. 1992. Glycosphingolipid phase behavior in unsaturated phosphatidylcholine bilayers: a ^{2}H-NMR study. *Biochim. Biophys. Acta.* 1106:85–93.

Neuringer, L. J., B. Sears, and F. B. Jungalwala. 1979. Deuterium NMR studies of cerebroside-phospholipid bilayers. *Biochim. Biophys. Acta.* 558:325–329.

Nieva, J. L., R. Bron, J. Corver, and J. Wilschut. 1994. Membrane fusion of Semliki Forest virus requires sphingolipids in the target membrane. *EMBO J.* 13:2797–2804.

Pascher, I., and S. Sundell. 1977. Molecular arrangements in sphingolipids: the crystal structure of cerebroside. *Chem. Phys. Lipids.* 20:175–191.

Pascher, I., M. Lundmark, P.-G. Nyholm, and S. Sundell. 1992. Crystal structures of membrane lipids. *Biochim. Biophys. Acta.* 1113: 339–373.

Pearce, P. A., and H. L. Scott. 1982. Statistical mechanics in the ripple phase of lipid bilayers. *J. Chem. Phys.* 77:951–958.

Pink, D. A., A. L. MacDonald, and B. Quinn. 1988. Anisotropic interactions in hydrated cerebrosides: a theoretical model of stable and metastable states and hydrogen-bond formation. *Chem. Phys. Lipids.* 47:83–95.

Reed, R. A., and G. G. Shipley. 1987. Structure and metastability of *N*-lignocerylgalactosylsphingosine (cerebroside) bilayers. *Biochim. Biophys. Acta.* 896:153–164.

Reed, R. A., and G. G. Shipley. 1989. Effect of chain unsaturation on the structure and thermotropic properties of galactocerebrosides. *Biophys. J.* 55:281–292.

Rintoul, D. A., and R. Welti. 1989. Thermotropic behavior of mixtures of glycosphingolipids and phosphatidylcholine: effect of monovalent cations on sulfatide and galactosylceramide. *Biochemistry.* 28:26–31.

Ruocco, M. J., G. G. Shipley, and E. Oldfield. 1983. Galactocerebroside-phospholipid interactions in bilayer membranes. *Biophys. J.* 43:91–101.

Rüppel, D., and E. Sackmann. 1983. On defects in different phases of two-dimensional lipid bilayers. *J. Physique.* 44:1025–1034.

Sackmann, E. 1994. Membrane bending energy concept of vesicle- and cell shapes and shape-transitions. *FEBS Lett.* 346:3–16.

Sackmann, E., D. Rüppel, and C. Gebhardt. 1980. Defect structure and texture of isolated bilayers of phospholipids and phospholipid mixtures. *In* Liquid Crystals of One- and Two-Dimensional Order, Vol. 11. W. Helfrich and G. Heppke, editors. Springer Series. 309–326.

Sargiacomo, M., M. Sudol, Z.-L. Tang, and M. Lisanti. 1993. Signal transducing molecules and glycosyl-phosphatidylinositol-linked proteins form a caveolin-rich insoluble complex in MDCK cells. *J. Cell Biol.* 122:789–807.

Schoen, P. E., R. R. Price, J. M. Schnur, A. Gulik, and T. Gulik-Krzywicki. 1993. Formation of lipid tubule microstructures: time-resolved freeze-fracture and x-ray characterization. *Chem. Phys. Lipids.* 65:179–191.

Schnur, J. M. 1993. Lipid tubules: a paradigm for molecularly engineered structures. *Science.* 262:1669–1676.

Siefert, U. 1993. Curvature-induced lateral phase segregation in two-component vesicles. *Phys. Rev. Lett.* 70:1335–1338.

Sternberg, B. 1992. Freeze-fracture electron microscopy of liposomes. *In* Liposome Technology, 2nd ed, Vol 1. G. Gregoriadis, editor. CRC Press, Boca Raton, FL. 363–383.

Suzuki, K., and Y. Suzuki. 1989. Galactosylceramide lipodosis: globoid cell leukodystrophy (Krabbe disease). *In* The Metabolic Basis of Inherited Disease II, 6th ed. C. M. Scriver, A. L. Beaudet, W. S. Sly, and D. Valle, editors. McGraw-Hill, San Francisco. 1699–1720.

Thompson, T. E., and T. W. Tillack. 1985. Organization of glycosphingolipids in bilayers and plasma membranes of mammalian cells. *Annu. Rev. Biophys. Biophys. Chem.* 14:361–386.

Thompson, T. E., M. Allietta, R. E. Brown, M. L. Johnson, and T. W. Tillack. 1985. Organization of ganglioside G_{M1} in phosphatidylcholine bilayers. *Biochim. Biophys. Acta.* 817:229–237.

Tillack, T. W., M. Wong, M. Allietta, and T. E. Thompson. 1982. Organization of the glycosphingolipid asialo-GM_1 in phosphatidylcholine bilayers. *Biochim. Biophys. Acta.* 691:261–273.

Vinson, P. K., J. R. Bellare, H. T. Davis, W. G. Miller, and L. E. Scriven. 1991. Direct imaging of surfactant micelles, vesicles, discs, and ripple phase structures by cryo-transmission electron microscopy. *J. Colloid Interface Sci.* 142:74–91.

Witter, B., H. Debuch, and H. Klein. 1980. Lipid investigation of central and peripheral nervous system in connatal Pelizaeus-Merzbacher's disease. *J. Neurochem.* 34:957–962.

Yao, H., S. Matuoka, B. Tenchov, and I. Hatta. 1991. Metastable ripple phase of fully hydrated dipalmitoylphosphatidylcholine as studied by small angle x-ray scattering. *Biophys. J.* 59:252–255.

Yunis, E. J., and R. E. Lee. 1970. Tubules of globoid leukodystrophy: a right-handed helix. *Science.* 169:64–66.

Zasadzinski, J. A. N., and M. B. Schneider. 1987. Ripple wavelength, amplitude, and configuration in lyotropic liquid crystals as a function of effective headgroup size. *J. Physique.* 48:2001–2011.